IUST
Iran University of Science and Technology

Iranian Journal of Electrical and Electronic Engineering

Journal Homepage: ijeee.iust.ac.ir

A Review of Ultrasound Imaging Methods and Techniques to Enhance Their Frame Rate

Seyyedeh Ensiyeh Hashemi* and Hamid Behnam*(C.A)

Abstract: Increasing the frame rate of ultrasound imaging while keeping image quality is important for following fast movements, especially the heart. There are different modalities for B-mode image recording, including line-by-line scanning with linear, phased, convex array, synthetic aperture imaging (STA), plane waves (PWI), then the combination of plane waves (CPWI), and so on. Researchers have tried to increase the frame rate in each case using different methods. Three approaches for this aim are data acquisition, post-processing, and beamforming. This article reviews these approaches and their solutions for compensating image quality reduction. Ultrafast ultrasound imaging, which provides exceptional temporal resolution (high frame rate), is promising in diagnosing heart diseases due to its ability to capture rapid heart movements. It can record images faster than conventional imaging, usually exceeding 1000 frames per second. This can be achieved through plane wave imaging (PWI). However, high frame rate data acquisition can lead to a decrease in image quality. Transmitting at different angles and then combining plane wave imaging is a popular method to enhance PWI quality but reduces the frame rate by the number of angles. As a result, researchers have aimed to increase the temporal resolution while compensating for the loss of quality.

Keywords: ultrasound, conventional imaging, plane wave imaging, neural network, frame rate, beamforming.

1 Introduction

ULTRASOUND waves are used in medicine for diagnostic purposes, as well as for therapeutic applications. Medical imaging through this method is performed in a non-invasive and secure manner. Using ultrasound to produce medical images is called sonography or echography. Sound waves are classified according to frequency into infrasonic (infrasound), whose frequency is below the limit of human hearing; acoustic (auditory), whose frequency falls within the range of human hearing; and ultrasonic (ultrasound), whose frequency is higher than the range of human hearing (more than 20000 Hz) [1]. In diagnostic medical applications, ultrasound waves from 1 MHz to 18 MHz are commonly used. Higher frequencies require smaller transmitter dimensions, and the shorter wavelength enables higher resolution. However, the amount of signal attenuation in the propagation environment rises with increasing frequency. The speed of sound is varies in different tissues, and it is typically considered to be 1540 m/s for soft tissues. At each emission (from one or more probe elements, depending on the imaging method), the reflections are received as a data vector by all the active elements of the transducer (probe). Then, by applying processing, radio frequency (RF) lines are created to generate the image. RF lines are positioned next to each other and displayed as a single image or consecutive frames. There exist several types of ultrasound transducers including linear, convex, and phased array. These transducers differ in their crystal arrangement, size, and footprint, which decide their suitability for various imaging applications. B-mode ultrasound imaging can be performed using various techniques, including traditional line-by-line scanning with linear, phased, and convex arrays, as well as more

Iranian Journal of Electrical & Electronic Engineering, 2025.
Paper first received 23 Dec. 2024 and accepted 17 Mar. 2025.
* The Department of Biomedical Engineering, School of Electrical Engineering, Iran University of Science and Technology, Tehran, 1684613114, Iran.
E-mail address: behnam@iust.ac.ir, ensiyeh_hashemi@elec.iust.ac.ir
Corresponding Author: Hamid Behnam.

advanced methods such as synthetic aperture imaging (STA) and plane wave imaging (PWI). A further enhancement of PWI is coherent plane wave compounding (CPWI), which improves image quality by integrating frames into multiple angles. Despite these advancements, achieving high frame rates while maintaining image quality remains a key challenge in ultrasound imaging. To address this, researchers have explored different strategies, which can be broadly categorized into three main areas: optimizing data acquisition protocols, applying advanced post-processing techniques, and improving beamforming algorithms. Each of these approaches contributes to enhancing temporal resolution and overall imaging performance, making them essential for real-time applications such as echocardiography.

Ultrasound imaging faces the challenges of image quality and imaging speed, especially in moving tissues imaging such as the heart. Being able to decrease the recording time for each image in a sequence is important for accurately tracking rapid cardiac movements, especially in the case of pulmonary and aortic valves, to diagnose heart problems. Frame rate is important in other applications such as blood flow imaging, kidney perfusion, and photoacoustic imaging. Medical ultrasound scanners are also capable of real-time blood flow visualization within the body. Doppler systems enable flow assessment at specific locations, providing detailed velocity distribution over time. Additionally, they generate dynamic color images of velocity at frame rates of up to 20–60 frames per second. If the frame rate is too low, rapid changes in blood flow velocity such as transient reverse flow components, may not be accurately detected, so frame rates as high as 100-200 per second would be needed [2,3]. Kidney perfusion refers to the blood flow through the kidneys, and limited frame rates can result in undersampling of faster flow regions, particularly in the renal cortex. High-frame-rate ultrasound enables power Doppler imaging, where the temporal incoherence of microbubbles facilitates the separation of contrast signal from tissue [4]. Photoacoustic tomography (PAT) is a noninvasive imaging technique that combines optical and ultrasound methods. By irradiating a sample with laser pulses, temperature rise results in generating pressure waves, which are then detected by ultrasound transducers to reconstruct an optical absorption map, providing high spatial resolution and soft tissue contrast at greater depths than pure optical imaging [5,6]. The ability to acquire high frame rate PA images enables applications like monitoring heart valve motion, myocardial function, and circulating tumor cells in blood vessels, which makes real-time Photoacoustic imaging a valuable tool for various biomedical applications.

For such applications, as well as elastography which requires many images in the shortest time possible (approximately 150 images for the heart and 1000 images for elastography per second), plane wave imaging is used. The images must have a desirable quality for proper diagnosis, including resolution and contrast. However, plane wave imaging has the lowest quality among imaging methods due to its transmission and reception from all elements and lack of focus. A modified method is the combination of plane waves, which are transmitted at different angles. This, however, reduces the frame rate according to the number of angles.

In the following sections, we first provide a brief discussion on the fundamental principles of conventional and STA imaging techniques in Sections 2,3. Subsequently in each section, techniques designed to enhance the frame rate for the corresponding imaging method are introduced. Section 4 covers the PWI imaging method, followed by CPWI. Section 5 explores the application of neural networks in high frame rate imaging. Subsequently, in Section 6, we discuss the presented approaches, and finally, in Section 7, we conclude the study.

2 Conventional Imaging

Linear arrays can generate rectangular images that cover a specific region of interest (ROI). In cases where the elements are situated on a convex surface, a smaller array can be used to extend the scanning area and get an image with a polar cross-section. The method of transmitting and receiving signals is like a linear array, involving the use of a considerable number of elements (typically between 128-256). Due to their size, convex and linear arrays are not suitable for heart imaging from between the ribs. A phased-array system using a smaller structure can be used instead, by acquiring an image with a polar cross-section using a transducer with a small footprint. The signals are electrically delayed for steering the direction of the beam [7].

In conventional imaging, a focused beam is produced to form each line of data, referred to as a scan line, by activating a group of transducer elements through pulsing. This group of elements is called an aperture, and they receive echo signals. The aperture is then moved by one or more elements and the pulsing is repeated to create another scan line. This process is repeated (N - A + 1) times and creates (N - A + 1) scan lines, where N is the total number of transducer elements and A is the number of elements in the aperture. Echo signals enter the beamforming operation to produce an RF line. Beamforming differs from one imaging technique or application to another. The most well-known beamforming methods are delay and sum (DAS) and minimum variance (MV). The final image is

obtained by collecting the RF lines in a single matrix, extracting the envelope using the Hilbert transform, and logarithmic compression (Fig. 1). This compression is necessary for dynamic range reduction of the echo signals.

Increasing the aperture size helps improve the lateral resolution of the image. This is because both the beam width at the focal point and the beam divergence angle are inversely proportional to the aperture width [8]. The noise level is also related to the aperture size, as a larger aperture provides more data for beamforming and helps reduce noise. However, the width of the resulting image is inversely proportional to the aperture size. Using larger apertures reduces the number of scan lines and, as a result, the width of the image decreases. Therefore, in conventional imaging, a balance between imaging quality and image width must be considered.

The frame rate depends on the maximum imaging depth and the number of scan lines and is calculated by the (1), Berkov (2011), [9]:

$$\mathrm{FR}_{\mathrm{conventional\_imaging}} = \frac{1}{\mathrm{NT}}, \mathrm{T} = \frac{2\mathrm{D}}{c} \rightarrow \mathrm{FR} = \frac{c}{2\mathrm{ND}} \quad (1)$$

Where *FR* is the frame rate and *N* is the number of scan lines. *T* or *PRP* (pulse repetition period) is the time interval between two consecutive pulse transmissions. *D* is the maximum imaging depth and *c* is the speed of sound in the imaging medium.

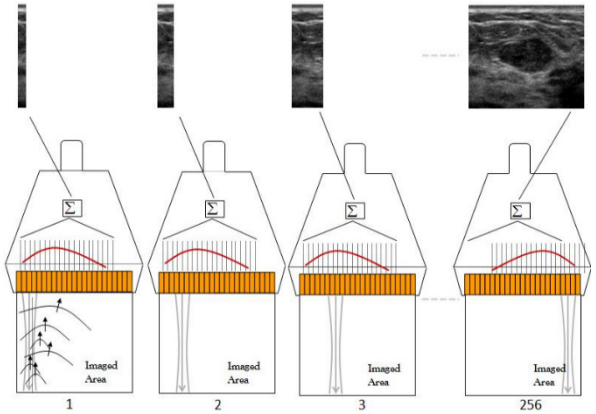

Fig 1. Schematic of line-by-line imaging with a linear array [9].

2.1 Increasing Frame Rate in Conventional Imaging

According to Eq.(1), the frame rate can be improved as bellow, but has limitations:

(1) Reducing the depth of penetration, as the pulses travel a shorter distance.

(2) Reducing the number of focal points, as fewer scan lines are needed.

(3) Reducing the number of scan lines.

Table 1 Shows the required speeds for different applications. Typical frame rates for 2D and 3D echocardiography systems are approximately 30–60 frames per second and 10–20 volumes per second, respectively [8]. This speed limitation has prompted researchers to develop methods for enhancing frame rate.

Table 1. Table 1 Examples of frame rates in various clinical applications for both conventional and ultrafast imaging [9].

Application	Typical imaging depth	Conventional architecture	Ultrafast architecture
Abdominal imaging	20 cm	20 Hz	3800 Hz
Cardiac Imaging	15 cm	150 Hz	5000 Hz
Breast imaging	5 cm	60 Hz	15000 Hz

There are three approaches for increasing the frame rate in ultrasound imaging:

•The first approach is based on data acquisition.

•The second approach is based on post-processing methods.

•And the third approach is based on beamforming.

The fundamental methods in the first approach involve reducing the viewing angle or decreasing the number of recorded lines in a frame. In the second approach, processing occurs after data acquisition, and in beamforming methods, efforts have been made, particularly for the minimum variance method, to increase the frame rate by reducing time/computational complexity.

Multi-line transmission (MLT) and acquisition (MLA) are one of the first methods, initially introduced by Mallart and Fink (1992) and Shattuck et al. (1984) [10,11]. MLA (also known as parallel receive beamforming) faces issues of reduced image resolution, increased side lobes, reduced penetration, and increased hardware complexity. In MLT, ultrasound pulses are simultaneously transmitted in multiple directions and can be combined with parallel receive beamforming to achieve a 12-16x frame rate (approximately 340-450 Hz) without significantly compromising the spatial resolution and signal to noise ratio. However, the limitation of MLT is the occurrence of crosstalk artifacts between parallel transmission beams, where the energy of the main lobe of a transmitting beam is received by the side lobe of another receiving beam, thereby decreasing the spatial resolution. These two methods are shown in Fig. 2. Research has been conducted to reduce the effects of these artifacts using different beamformers [12].

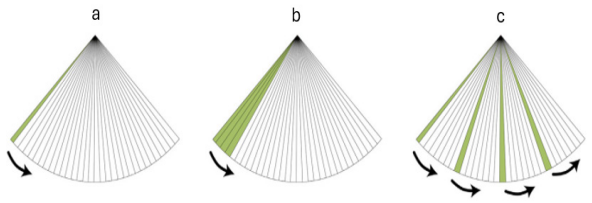

Fig 2. The figure shows three different image scan schemes. Conventional beam forming (single line acquisition) is shown in A. B shows multiline acquisition (e.g., 4 multiline acquisition). C shows multiline transmit (e.g., 4 multiline transmit). The arrows indicate the direction of the scanning process [12].

Retrospective gating was one of the earliest approaches [12] used for achieving high-speed imaging while preserving spatial resolution and field of view. In this approach, a large imaging section is divided into several small sub-sections. Each of these sub-sections is imaged with a high frame rate, based on its limited field of view, during one cardiac cycle. Using retrospective electrocardiogram (ECG) gating, sub-segment images are then combined to produce images of the entire imaging segment. However, the ECG gate may not be effective if the heart rate varies during different cardiac cycles. In such cases, motion matching serves as an alternative method for combining sub-images. In this method, both neighboring subdivisions overlap slightly, and the local motion patterns extracted from these regions coincide temporally. The periodicity of the heartbeat is used for the temporal alignment of two neighboring subdivisions. In practice, a balance must be struck between the number of sub-segments to be combined and the resulting frame rate. In this scenario, each image line in the overlap region is imaged twice - once by the first transmission beam and once by the second beam. Unfortunately, this technique is not useful in cases of atrial fibrillation (an irregular and often abnormally fast heartbeat).

Wang et al. (2008) [13] developed an automatic method for multi-segment ultrasound imaging using ECG. This method involves employing seven different sectors at various angles, continuously acquiring seven ECG signals and seven RF signals for each sector, extracting one complete cardiac cycle from the ECG and RF frame signals, and combining the corresponding frames to create full-view ultrasound images. This method achieved a frame rate of 481 Hz at an imaging depth of up to 11 cm and a 100% field of view during breath-holding. The limitations of this method include the need for high accuracy in synchronizing the ECG with the recorded frames, and the fact that each section of the final frame may not necessarily correspond to a cardiac cycle, resulting in incorrect information display for those with irregular heartbeat or disease. Furthermore, ECG needs long acquisition times and is sensitive to any added motion that may occur during acquisition.

In another study conducted by Perrin et al. (2012) [14], two-dimensional echocardiographic images of periodic frames from several cardiac cycles were arranged to reconstruct a sequence with a higher frame rate. The order was based on the R wave peak obtained from the ECG. They assumed that an R peak would occur in the ECG waveform in the Kth frame. Therefore, that frame was considered for three heartbeats in the sequence of frames. Based on the occurrence time of the R peak, they were rearranged and placed in the sequence, and the process was repeated (Fig. 3). This method only uses repetitive information, and in cases where echocardiography is abnormal or patients have irregular heartbeats, it may require many intervals to reconstruct a higher frame rate movie or could even become impossible. This is because R peaks may not necessarily appear in the assumed frames.

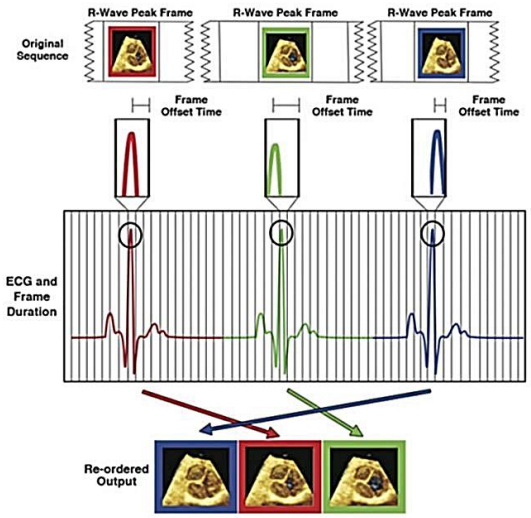

Fig 3. The schematic figure depicts an example of the proposed algorithm, where frames covering the duration of the ECG R-wave peak are reorganized according to their start time in relation to the peak's occurrence [14].

In the studies of Gifani et al. and Shalbaf et al. (2011, 2010, 2015) [15,16,17], a post-processing approach was taken where the manifold learning algorithm was applied to two-dimensional echocardiographic images to find the relationship between frames of a cardiac cycle. Each image is represented by a point in the reconstructed manifold (Fig. 4), [15]. There are three dense regions on the manifold that correspond to the three phases of the cardiac cycle (isovolumetric systole, isovolumetric relaxation, and reduced filling), in which there are no prominent changes in ventricular volume. Since the end-systolic and end-diastolic frames are in the same volume phases of the cardiac cycle, dense areas can be used to find these frames. The minimum correlation between

these images leads to the detection of end-systole and end-diastole frames. With the (Locally Linear Embedding) LLE algorithm, the nonlinear dimension has been reduced. The main advantage of the LLE algorithm is that similar frames in high-dimensional space keep their neighborhood in low-dimensional space. By identifying the relationship between frames and sorting the extracted images, they merged the three cycles into one cycle with more images, thus increasing the frame rate (Fig. 5) [15].

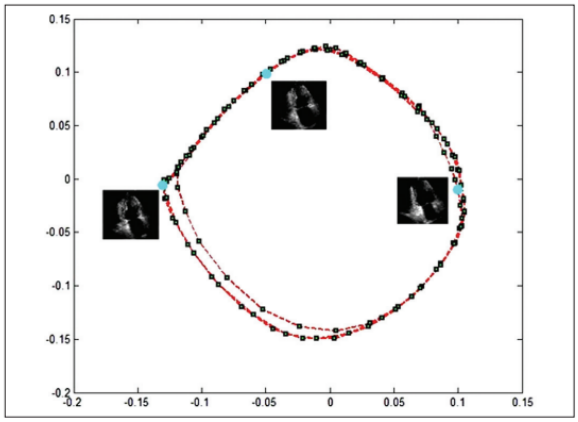

Fig 4. The LLE algorithm was used to perform a two-dimensional non-linear embedding of three cardiac cycles in normal hearts, with k=10 neighbors used during the process [15].

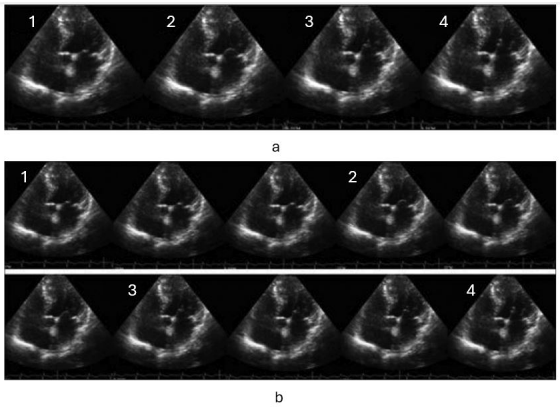

Fig 5. a) Four consecutive frames of the first cycle. b) Inclusion of two other heart cycles in the first cycle [15].

Based on the proposed method, only ultrasound images are needed and there is no need for an ECG recording system to be used alongside ultrasound imaging, as the images are extracted without ECG references. This can result in a more cost-effective cardiac ultrasound imaging device, and the imaging method becomes easier for patients and cardiologists due to not needing to take an ECG and the simultaneous use of other electrodes. Although the results show that the proposed method applies to normal cases, the algorithm may not be responsive to a wide range of abnormal cases (such as patients with arrhythmia, pathology, and ventricular ectopic beats).

Gifani et al (2015) [18] proposed another post-processing approach based on interpolation for achieving ultra-high temporal resolution in cardiac ultrasound imaging based on sparse signal representation and temporal information. The proposed method does not require training in low-resolution and high-resolution dictionaries, as well as motion estimation. The first step in this method involves extracting the intensity variation time curves (IVTCs), which are evaluated in each pixel of consecutive echocardiographic frames (Fig. 6). The predefined functions include four families of wavelets, along with sine and cosine functions, based on prior knowledge of the nature of IVTC signals. By having initial sparse coefficients for the IVTC signal with T samples, new sparse coefficients are created for the new IVTC signal with T^' samples (Fig. 7). The figure shows an increase up to a 3-fold ratio. The main limitation of this method is its computational complexity compared to other methods.

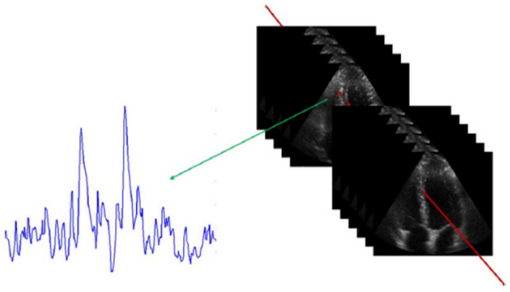

Fig 6. IVTC curve of one pixel in (x, y) coordinates extracted from all frames [18].

One of the post-processing methods is frame rate up-conversion (FRUC), in which extra frames are interpolated and inserted between two consecutive frames. Many FRUC algorithms use motion estimation and motion-compensated frame interpolation. Motion estimation techniques in echocardiography use speckle tracking methods or matching the images to the base image (nonrigid image registration) of the spatial-temporal deformation field, which effectively estimates the motion by minimizing the difference, Alessandrini et al. (2014, 2016) [19,20]. However, in low frame rate imaging, speckle noise and large motions between two consecutive frames make motion estimation difficult. Furthermore, in heart diseases and irregular heartbeats, it may not be estimated correctly.

In the study of Mirarkolaei et al. (2020) [21], a variable bidirectional motion estimation model is proposed for motion-compensated frame interpolation.

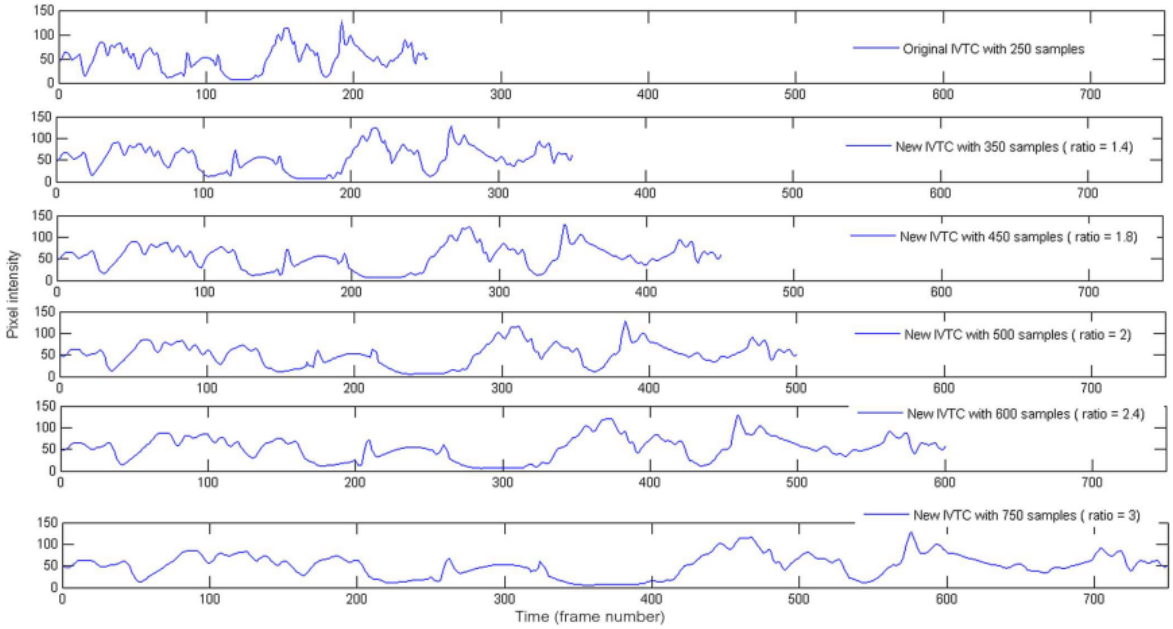

Fig 7. The result of the method proposed in [18] create new IVCTs with different ratios: 1.4, 1.8, 2, 2.4, and 3

The Euler-Lagrange equations that characterize the optimal two-dimensional dense motion field are derived and a multiscale iterative method is developed to obtain the motion field and missing intermediate frames. Experimental results show that the proposed algorithm produces interpolation frames without the commonly present blurring artifacts in existing motion-compensated frame interpolation algorithms. Fig. 8 shows the interpolation between two consecutive frames.

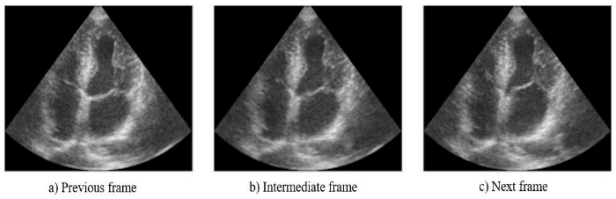

Fig 8. (a)–(c) shows three consecutive frames with an interpolation between the two frames during end systole and early diastole before mitral valve opening [21].

Jalali et al (2020) [22] also used IVTC signal for 3D imaging. The frame rate limitation in 3D echocardiography is worsened as it must scan a volume instead of a plane, which takes more time compared to 2D mode. In this study, a time interpolation method using B-splines has been suggested, which is more efficient than the sparse representation method in terms of both error rate and computational complexity. The choice of dictionary atoms in the sparse representation method, by which the IVTC signals must be approximated as a linear combination of atoms, can cause this difference. Cubic B-Spline super resolution provides excellent performance in increasing frame rate and improving image quality. Image quality metrics, such as contrast-to-noise ratio, show that the image is improved in interpolated frames as the frame rate increases. In 3D echocardiography, due to the lack of temporal information, frame rate enhancement is not performed as in 2D mode, and fewer frames result in mistaken interpolation of 3D IVTCs. The paper shows that cubic B-Spline has lower errors in reconstructing both 2D and 3D echocardiographic IVTCs compared to other B-Spline interpolations. Therefore, cubic B-Spline is the preferred interpolation method.

In another study by Jalali and Behnam (2021) [23], it was proposed to increase the number of frames in 3D echocardiography sequences to enhance the accuracy of tracking endocardial surface spots. It was shown that using IVTC curves and cubic B-spline interpolation helped improve tracking accuracy compared to the original sequences. The results show that employing the proposed method can help the tracking algorithm perform better and follow spatial patterns more accurately. This is because in fast-moving organs such as muscles and heart valves, the speckle pattern constantly changes, and the tracking algorithm must adjust to new patterns in almost every new frame.

Afrakhteh et al (2022) [24], have proposed a non-polynomial interpolation method to increase the frame rate in echocardiography. Since the parts that move faster in echocardiography are crucial for medical diagnoses, more specialized bases than traditional polynomial bases should be used. Polynomial bases

produce larger errors in parts of the data with large variations. The primary findings of the article are as follows: First, non-polynomial interpolation performs better than polynomial interpolation in dealing with non-smooth data. Second, since these non-polynomial functions are based on continuous and infinitely differentiable functions, they also keep their smoothness properties. Another advantage is that the proposed method can increase the temporal resolution of echocardiographic images up to 4-fold without reducing image quality. In another study by this group (2023) [25], a spatial-temporal numerical method based on two-dimensional interpolation is proposed. Specifically, a new strategy called Intensity Variation Time Surface (IVTS) is proposed to combine temporal and spatial information in the reconstruction. In this method, first, IVTS is extracted based on data collected from different rows of all sample frames. Then, intermediate interpolated frames are created by reconstructing the missing information of IVTSs using 2D interpolation. The proposed 2D interpolation reduces reconstruction errors by extending the concept of IVTC to IVTS while keeping the helpful features of earlier IVTC-based methods. In this regard, radial basis functions (RBFs) have been used for two-dimensional interpolation. RBFs are chosen because they can interpolate on large-scale datasets, and their mathematical implementation is simple. Another important feature of this interpolation technique is its meshless nature, which allows for higher sampling rates in echocardiography to improve temporal resolution without a significant reduction in image quality. To assess the proposed method, RBF interpolation was evaluated on 2D/3D echocardiography datasets. Fig. 9 shows two examples of original frames compared to frames reconstructed using the proposed technique.

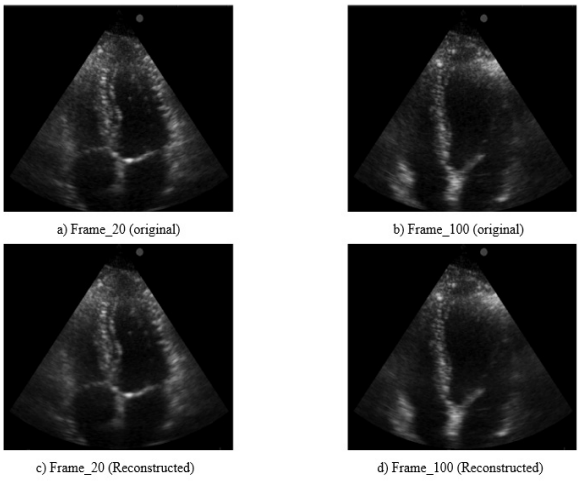

Fig 9. The first row illustrates the original frames, and the second row displays the reconstructed frames using the proposed interpolation techniques [25].

In the work of Hosseinpour et al (2019) [26], compressed sensing (CS) is used for temporal resolution improvement. In compressed sensing, instead of sampling from a signal, measurements are taken from the signal. The number of measurements needed for signal recovery in compressed sensing is much lower than the number of samples needed for signal recovery according to the Nyquist theorem. For example, for an audio signal with a bandwidth of 4 kHz, the Nyquist theorem dictates that the sampling rate must be at least 8 kHz for full signal recovery; however, the audio signal is sparse in the short-time Fourier transform (STFT) domain, meaning that many of its STFT coefficients are zero. CS is an acquisition method in which only a few randomly selected samples of a signal are measured blindly, and the complete signal is reconstructed under certain conditions. The schematic of the proposed method is shown in Fig. 10. Data sparsity is considered in both spatial and temporal directions in RF signals and intensity-time curves (IVTCs), respectively, and CS reconstruction is applied in both spatial and temporal directions. Using this method, the frame rate of ultrasound imaging can be increased by up to two times. Fig. 11 shows reconstructed images using the proposed methods. The drawback of the CS method is its extremely high processing time.

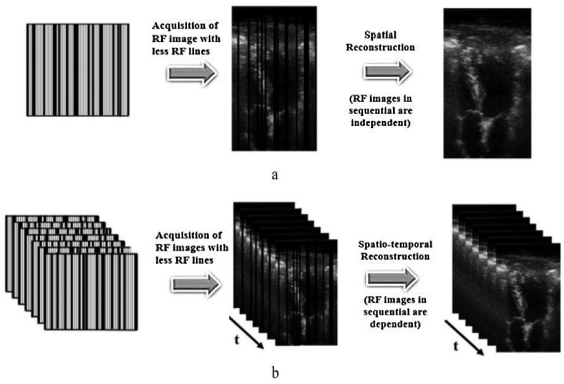

Fig 10. methods of image reconstruction on a 2D ultrasound RF image sequence with a line-wise pseudo-random sampling mask. (a) using conventional CS reconstruction, (b) proposed CS reconstruction approach in the Spatial-Temporal domain [26].

In a line-by-line imaging system, the frame rate is dependent on the number of scan lines. Hence, if a fraction of lines is collected and other lines are estimated in the original image, the frame rate can be increased.

Afrakhteh and Behnam (2020) [27] have proposed a data acquisition technique to estimate the RF data matrix using DCT-based reconstruction. Although compressed sensing provides a high-accuracy reconstruction of the original signal, its main limitation is a significant increase in computational complexity. Therefore, a

DCT-based method for reconstructing unformed lines with MV (only 33% of lines took part in the beamforming process) is presented with extremely low complexity. Fig. 12 shows the comparison of different methods for beamforming.

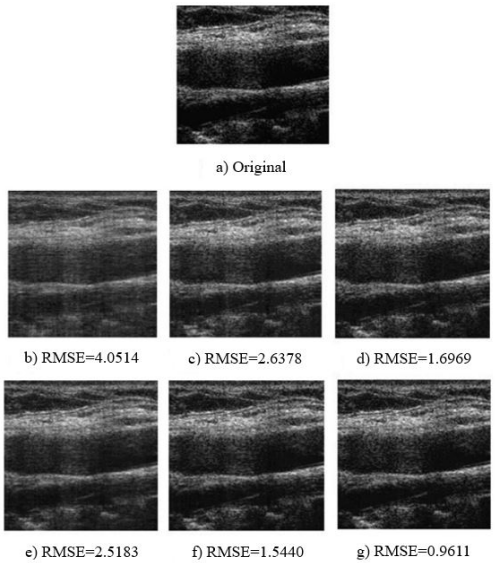

Fig 11. The reconstructed image from a 3D echocardiographic volume sequence using the proposed Spatial-CS and Spatial-Temporal-CS methods with complete temporal and spatial learned dictionaries is presented. The original image is shown in (a), and the reconstructed images using the Spatial-CS method are shown in (b-d), the images reconstructed using the Spatial-Temporal-CS method are shown in (e-g) for 25%, 50%, and 75% of the main lines, respectively [26].

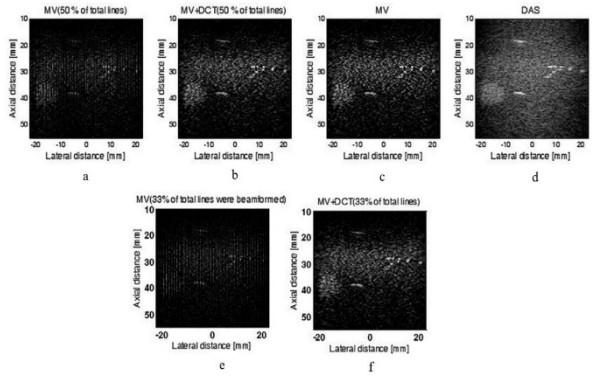

Fig 12. An experimental cyst phantom using a 128-element, 6 MHz linear array. a) RF lines were determined for beamforming (50% of total lines). b) MV + DCT (50% of total lines). c) MV (L = 64, Δ = 1/100 L). d) DAS. e) MV (33% of total lines). f) MV + DCT (33% of total lines) [27].

In another study (2020) [28], Hosseinpour et al, used the matrix completion method in their data acquisition approach, in which the problem is completing a low-rank matrix when only a subset of its elements is available. MC is an extension of CS for recovering two-dimensional signals. The first rows of each RF image in the sequence form an MC image. Thus, the first row of the first RF image is the first row of the first MC image. The first row of the second RF image, the second row of the first MC image, and the first row of the T-th frame form the m-th row of the first MC image. Consequently, the first MC image is formed with T rows, which is equal to the number of RF images in the sequence. The number of columns in this MC image is equal to the number of RF lines in the image. This is performed for all rows of the RF image sequence (Fig. 13). This sequence can include several cardiac cycles. As the heart has periodic and repetitive movement in successive cycles, the cycles are like each other. Therefore, for the images obtained in a sequence (several cardiac cycles), most of the data or information are either the same or similar and the assumption of the low rank of the matrix is fulfilled. According to Fig. 14, the sequence of RF frames is reconstructed by the proposed method. The computational complexity of this method is much lower than CS, and the frame rate increases up to two times.

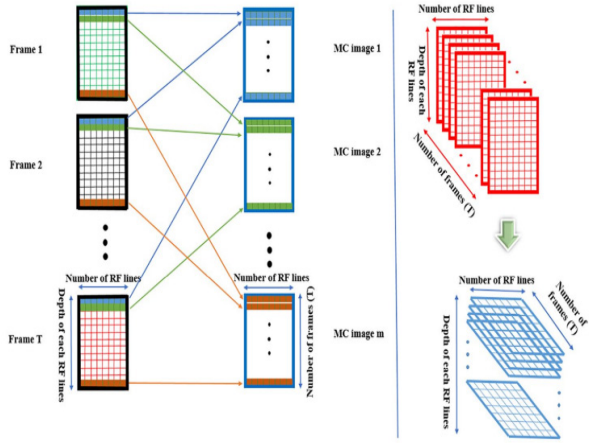

Fig 13. Schematic of how MC matrices are formed from RF data matrix rows [28].

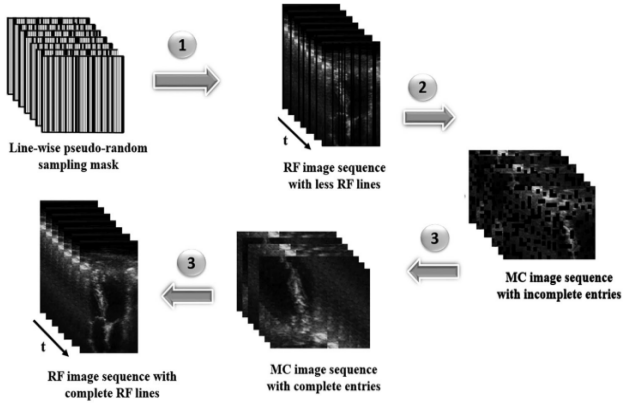

Fig 14. The proposed Spatial-Temporal-MC approach was employed for the reconstruction of an RF image sequence [28].

However, for ultra-fast movements, this value should still be higher. Fig. 15 shows reconstructed images from 2D carotid artery data using three reconstruction methods.

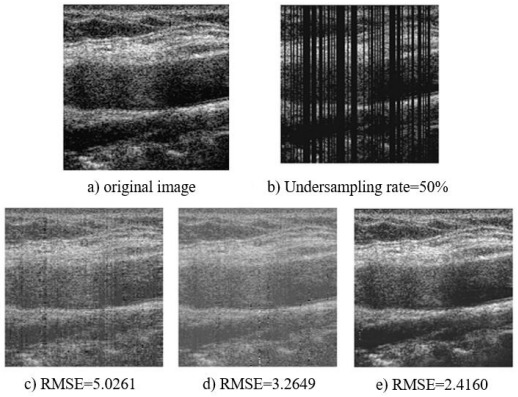

Fig 15. The reconstructed image from two-dimensional carotid artery data using three reconstruction methods is presented. The methods are as follows: (a) original image, (b) image from RF lines sampled at a sampling rate of less than 50%. Reconstructed images using (c) Spatial-CS, (d) Spatial-Temporal-CS, and (e) proposed Spatial-Temporal-MC methods [28].

3 Synthetic Aperture Imaging (STA)

Another type of imaging method is the synthetic aperture, in which the transmission is done sequentially by each element, and the reception is through all elements, as shown in Fig. 16, [29]. This method creates several images with low resolution which are then combined to create a final high-resolution image. The disadvantage of this method includes its computational cost and susceptibility to motion artifacts. This method achieves a higher frame rate compared to conventional approaches. However, for ultrafast applications, specific designs have been introduced, which will be discussed in the following.

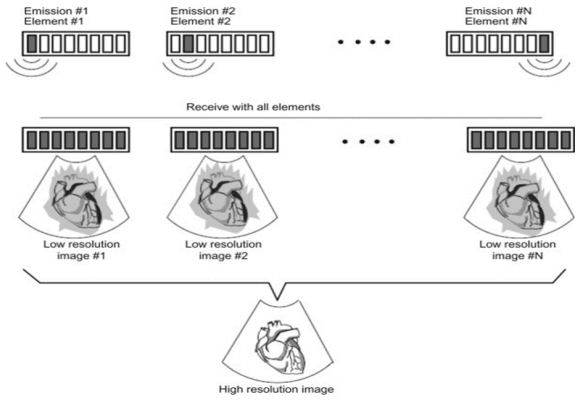

Fig 16. Schematic of synthetic aperture imaging method [29]

The TC algorithm is an extended version of the matrix completion algorithm that is widely used to solve problems related to large-scale matrices. It is often assumed that missing data entries depend only on their neighboring entries. Therefore, only a few neighboring inputs are used to estimate missing inputs. However, in some cases, missing entries do not only depend on neighboring entries but on the whole dataset. in other words, the dependency of missing inputs on existing data is general. In such cases, using all the available data to estimate the missing values leads to a more correct approximation. The TC algorithm is developed based on this idea, where the optimization problem is written in a way that all data is used to estimate the missing inputs. The higher the linear dependency between the matrix columns, i.e., the lower the matrix rank, the fewer columns are needed to retrieve other columns. The tensor rank is defined similarly. It can be concluded that for a low-rank tensor, its missing entries can be recovered by using a small number of existing entries. Therefore, the TC algorithm aims to minimize the tensor rank.

Afrakhteh and Behnam, in their study (2021) [30], focused on synthetic aperture (STA) imaging. In this imaging technique, each element is activated sequentially, and then all elements receive and make a low-resolution frame. Consequently, the frame rate is dependent on the number of array elements, because all elements must be activated individually to form a single frame. Although acceptable image quality is obtained in the STA method, it is not efficient in terms of time and provides a limited frame rate depending on the number of array elements. To this end, their study introduced a novel approach, which randomly selects M/L elements instead of using all M elements and reconstructs the remaining frames using the tensor completion method, leading to a significantly higher quality image with a 3-fold increase in frame rate. The proposed method is shown in Fig. 17.

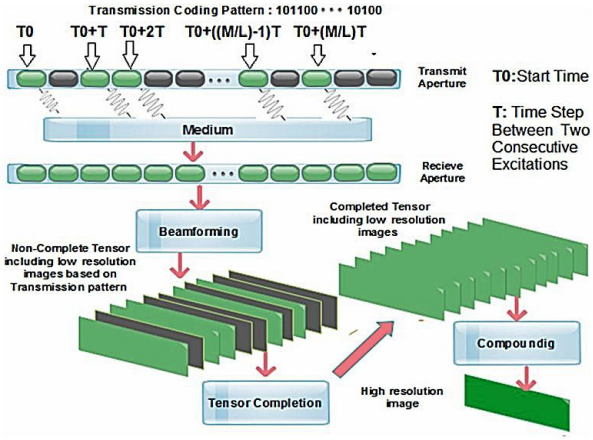

Fig 17. The proposed STA is illustrated in the diagram. The unknown data is represented by the black color in the tensor [30].

In another research, Afrakhteh et al. (2022) [31], performed this process for the phased array probe and echocardiographic images. This time, some scan lines were not registered in the phased array, and by completing the tensor, it recovered the unregistered lines, and the frame rate increased up to 4 times.

4 Plane Wave Imaging (PWI)

Ultrafast frame rates are essential for many ultrasound imaging applications. This is necessary for detecting the movement of a specific target, such as heart rate during the cardiac cycle, determining blood flow velocity, and tracking shear wave propagation in elastography [32].

Elastography is a technique for measuring tissue stiffness. In elastography by compressing the desired tissue and imaging it before and after compression the elasticity of the tissue can be measured. Compression can be done dynamically by generating shear waves that propagate through the tissue, which is called shear wave imaging. Ultrafast imaging techniques are needed to image the tissue particles in this method. Shear waves suffer from much stronger attenuation effects. They travel at a speed of 1 to 10 meters per second and have a low frequency of 50 to 500 Hz. Therefore, tracking shear waves in tissues requires imaging at a frame rate of 1000 frames per second to maintain the minimum limit of Nyquist sampling rate [33]. Achieving a super high frame rate of thousands of frames per second is not possible without using plane wave imaging. Plane-wave imaging is a type of imaging that uses an unfocused beam to view the imaging area. While a single transition in linear imaging creates a scan line, PWI produces a complete image with a single transition. To form a single frame in PWI, all elements in the transducer are activated simultaneously and then used to receive the reflected echoes from the observation points. Therefore, PWI can have a high frame rate, which is equal to the frame rate of linear imaging multiplied by the number of scans lines and is usually several thousand frames per second [9]. A schematic of this method is shown in Fig. 18.

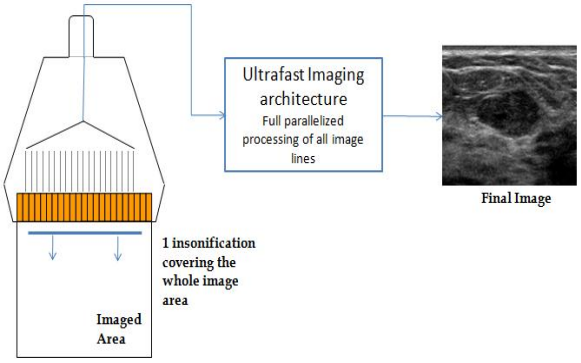

Fig 18. Schematic of plane wave imaging (PWI) [9]

4.1 Compound Plane Wave Imaging (CPWI)

Due to the lack of focus in PWI and the use of a transmitted pulse to image the target area, the quality of imaging is usually reduced in terms of resolution, side lobes, and contrast. One of the most popular techniques for improving the quality of PWI is compound plane wave imaging (CPWI). Instead of forming an image with a single transmission in PWI, CPWI produces an image by combining several images as in Fig. 19, each of which is produced by directing the unfocused beams at a specific angle.

The frame rate achieved in CPWI is the frame rate for a single plane wave divided by the number of compound angles as (2):

$$\mathrm{FR_{CPWI}} = \frac{\mathrm{FR_{PWI}}}{N_A} \tag{2}$$

FR_{PWI} is the frame rate for a single plane wave and N_A is the number of compound angles. This frame rate is suitable for ultrafast imaging applications in specific numbers of angles. The maximum number of compound angles can be estimated based on the imaging depth, speed of sound, and tissue movement in the target area.

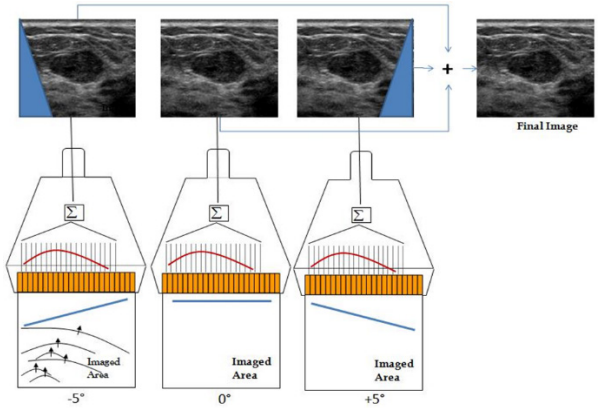

Fig 19. Schematic of the CPWI imaging method and combining images produced at different angles [9].

Berkov (2011) [9], explained the minimum frame rate necessary for recording shear wave propagation in human tissue. To keep this frame rate when using CPWI, no more than 3, 5, and 15 frames can be combined during abdominal, heart, and breast imaging, respectively. When using CPWI for such applications, e.g., shear wave imaging that requires at least 1000 to 4000 frames per second, the required imaging quality must be achieved using the minimum possible number of composite signals. This needs an understanding of the impact of the number and values of the composite angles on the spatial resolution and side lobe levels to ease the choice of suitable angles. Therefore, a method for calculating the optimal angles is necessary to achieve the best possible imaging quality using the minimum number of frames.

Afrakhteh and Behnam, implemented the tensor completion (TC) method for CPWI imaging (2021) [34] where instead of transmitting at 75 angles, which results in a lower frame rate, some angles were randomly removed. By completing the tensor information, the unrecorded angles were recovered. Using 20% coherent plane waves and reconstructing the remaining 80% via TC, they achieved image quality closely resembling the use of all 75 angles, with a resolution difference of less than 2%. Fig. 20 shows the proposed method. Black plates are frames that were not captured at random angles. In other studies, Afrakhteh et al. [35,36], unsent angles in CPWC were reconstructed using two-dimensional spatial-angular interpolation. Radial basis functions (RBF) were used for two-dimensional interpolation due to their flexibility, mathematical simplicity, and ability to prevent overfitting (which can occur with techniques such as polynomial interpolation). Fig. 21 displays simulated cyst targets at 5 and 15 angles with and without TC.

Paridar and Mohammadzadeh Asl, (2023) [37], proposed an MV algorithm based on tensor completion (TC) to simultaneously improve frame rate and image quality in CPWC. In this method, the MV algorithm is applied to a limited number of pixels. Then, using the TC algorithm, suitable values are assigned to the unprocessed pixels (Fig. 22). According to the authors, the proposed algorithm speeds up the beamforming process and thus improves the frame rate. The results show that by processing 40% of the data using the MV beamformer followed by the TC algorithm, a reconstructed image comparable to the case in which the MV algorithm is performed on the full data is obtained. To improve image quality compared to the conventional DAS algorithm, the adaptive MV algorithm was proposed for limited pixels of the sparse grid for each emission. Since this algorithm is applied to a small number of pixels, the computation time will be much less compared to the MV beamforming time for a complete set. Fig. 23 shows a reconstructed image using DAS, MV, and TC-based MV with 40% grid pixels.

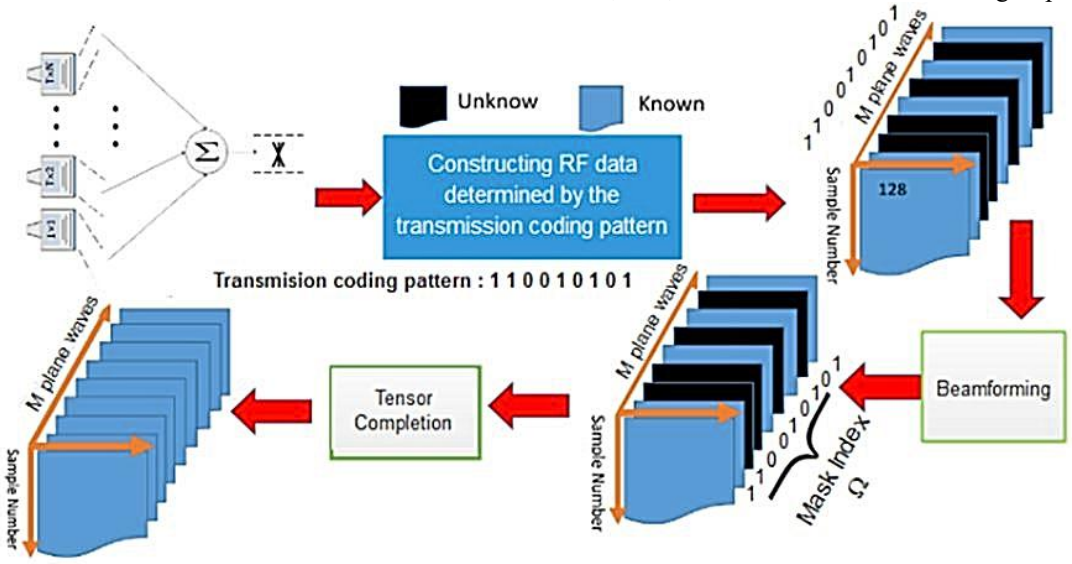

Fig 20. Schematic of the proposed method of CPWI imaging and tensor completion [34]

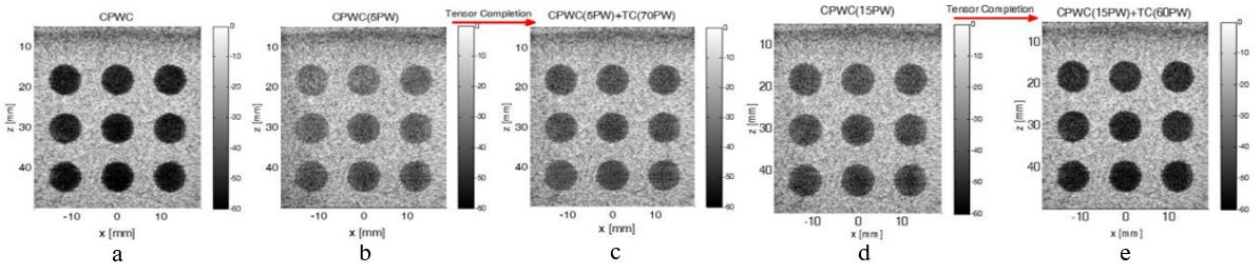

Fig 21. Image of cyst targets simulated by (a) CPWC (using 75PW), (b) CPWC (5PW), (c) CPWC (5PW) +TC (70PW), (d) CPWC (15PW), and (e) CPWC (15PW) +TC (60PW) [34]

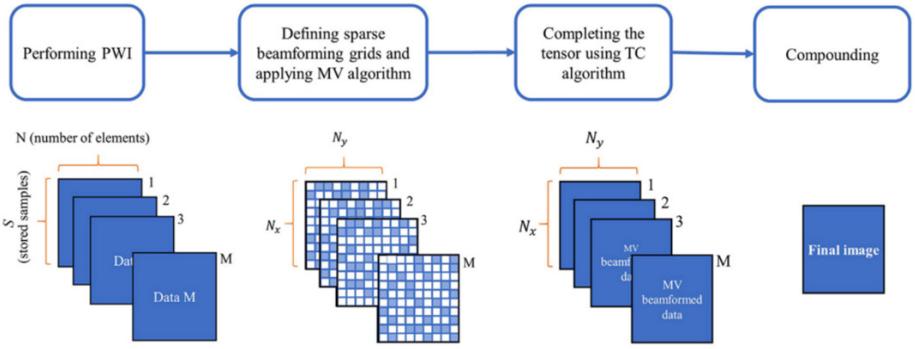

Fig 22. The steps of the proposed method in the figure can be described as follows: The received signal corresponding to each transmission is represented by an S × N matrix, where S is the number of samples for each element. A beamforming grid consisting of Nx × Ny pixels is defined in the region of interest, and then MV is used to process these matrices with discarded data [37].

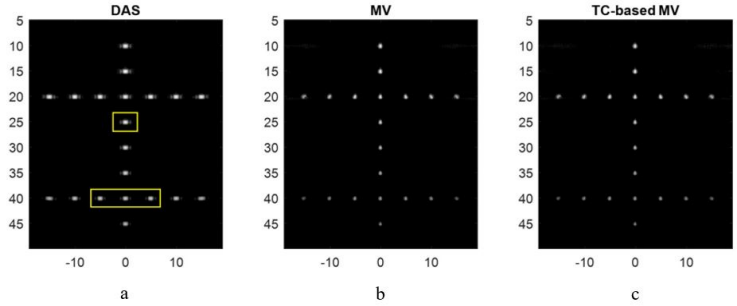

Fig 23. A reconstructed image of the simulation-resolution phantom was obtained using (a) DAS, (b) MV, and (c) a TC-based MV algorithm with 40% of grid pixels [37].

Another study by Paridar and Mohammadzadeh Asl, (2023) [38] reduced the number of angles using two sampling factors. More precisely, two different subsets, each consisting of a few transmits, were considered. The optimal values of angular distances are obtained based on the beam pattern that corresponds to the reference mode (that is, the case in which all plane waves are used). In the proposed algorithm, the delay and sum (DAS) beamformed images of the two subsets were combined to achieve the final reconstructed image. With this method, the required transmissions were reduced to 16, (Fig. 24). The larger the angular distance (i.e., dL), the better the resolution of the reconstructed image due to covering a wider range of the imaging area. However, the image contrast is reduced. On the other hand, by reducing the angular distance, the contrast of the image improves at the cost of resolution. To deal with these two, it was proposed to select two subsets of transmission angles, each consisting of M and N (integers) plane waves. According to the description in the article: $N=M=\sqrt{N_P}$, $d_N = d_L$, $d_M = Nd_L$, $N_P=75$. For the first subset, N transmissions are selected, which leads to good contrast. Also, for the second subset, the angular distance is multiplied by N. This means that M transmissions are selected with a greater angular distance than the first subset, resulting in good resolution. Finally, the results of the two sets are convoluted and the final image is made. Fig. 25 shows reconstructed images of phantom Simulation-Resolution, phantom Simulation-Contrast, phantom Experimental-Resolution, phantom Experimental-Contrast, and in-vivo data (last column). The first and second rows are related to the results of subset 1 and subset 2, respectively.

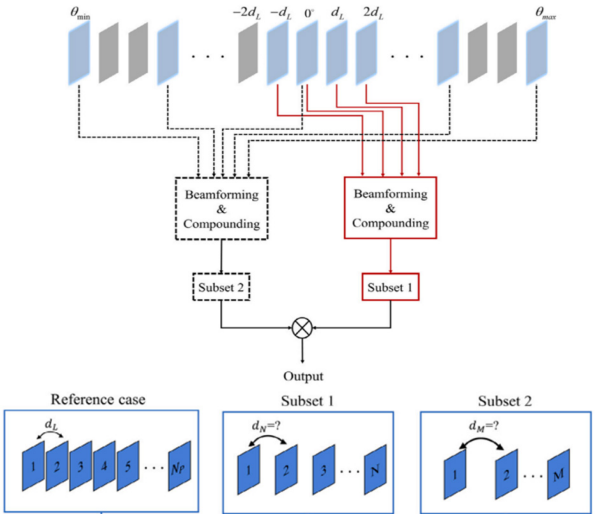

Fig 24. Schematic of the proposed method to increase the CPWI frame rate by reducing the number of angles [38]

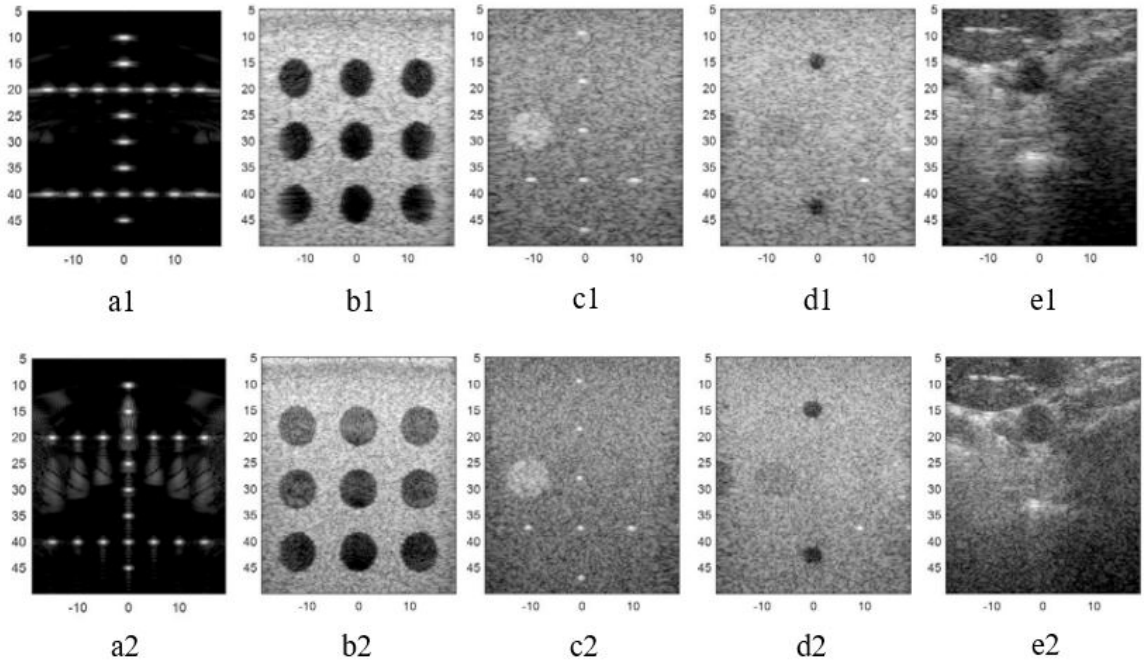

Fig 25. Reconstructed images from SR phantom (first column), SC phantom (second column), ER phantom (third column), EC phantom (fourth column), and in-vivo data (last column). The first and second rows are related to the results of subset 1 and subset 2, respectively [38].

5 Using Neural Networks in Image Enhancement and Beamforming in High Frame Rate Imaging

One of the areas that has received attention recently is the use of neural networks to increase the frame rate, beamforming, and improve the quality of images. The diagnostic reliability of PWI imaging is reduced by low-quality images. Medical ultrasound equipments on the market usually uses line-by-line scanning mode, which obtains high-quality images at a low frame rate. In addition, many proven data-based ultrasound image processing methods are taught by line-by-line scan images. In research by Zhou et al, (2019) [39], a network is proposed to improve the quality of PW images by reconstructing these images according to the line by line scan images. The gray level distribution of line-by-line scan images and PWI images are quite different, so the training pairs are not aligned, and the purpose of this paper is to solve the problem of low convergence of the network due to this difference. For this purpose, by organizing the sequence of the transducer array, it records the two pairs of images with the least difference. The proposed method obtains a linear scan quality image with an extremely high frame rate. The evaluation of the model was done with the PWI data set compared to the CPWI with a combination of 75 angles shaped by DAS. The network used in this work is based on the generative adversarial network (GAN). The GAN can be used to generate new samples that can be reasonably obtained from the original dataset. GAN consists of two neural networks, a generator G(x) and a differentiator D(x). Both play an adversarial game. The goal of the generator is to trick the discriminator by producing data like the data in the training set. The discriminator will try not to be fooled by finding fake data from real data. Both works simultaneously to learn and train complex data such as audio, video, or image files. As an example of image-to-image conversion, we can mention the conversion of summer to winter images and day to night images. These images are produced in such a way that even humans cannot tell that the images are fake. In the mentioned work, it has been tried to convert low-quality PWI images into line by line ones with the proposed method of GAN compared to other networks, for example, CNN.

In the study by Tang et al. (2021) [40], a GAN-based network is proposed to enhance the quality of PWI images. The network's weights are refined using full CPWI, resulting in high-quality image reconstruction. The discriminator calculates the difference and gives it to the network generator to modify the weights. The output for PWI images using a network is presented compared to CPWI with 3, 11, and 75 angles. The data used is from the PICMUS collection, which includes cases simulated with Field 2, experimental phantom, and in vivo of the human carotid.

So far, we have seen the use of neural networks trained with high-quality line-by-line scanning data, which can convert plane wave data into images comparable to line-

by-line scans. In the study of Wang et al. (2022) [41], the PWI imaging mode is fixed, but they trained the network with the data that has beamformed by MV and then obtained the same quality as MV from the data that has beamformed by DAS. The total training data of 200 frames includes 50 cases simulated with field 2, 50 cases from the experimental phantom and 100 in vivo data. The results of the three beamformers are shown in Fig. 26. The proposed method has comparable image quality, less computational complexity, and a faster frame rate compared to MV, as shown in Fig. 26 (c). In terms of computational complexity, MV requires 2.18 billion FLOPs to calculate the weights, and the proposed method requires 32.6 million FLOPs to form a scan line. The computational complexity of MV is about 67 times higher than the proposed method. In practice, the average execution time of MV is 6.02 seconds by CPU for one scan line and 0.9 ms for the proposed method with GPU. This leads to an increase in speed of about 3000 times [41]. By concurrent parallel processing of M scan lines via GPU, the frame rate of the proposed PWI beamforming can reach 1000 frame per second, which is sufficient for real-time PWI imaging [41].

A notable approach involves employing deep learning-based beamformers, such as U-Net and EfficientNet, to reconstruct high-resolution B-mode images from raw RF data. The study by Nguon et al. (2022) [42] introduced a modified U-Net architecture leveraging EfficientNet-B5 as the encoder and U-Net as the decoder, demonstrating significant improvements in lateral resolution, contrast-to-noise ratio, and peak signal-to-noise ratio compared to conventional delay-and-sum (DAS) and CPWC methods. The proposed model reduces computational complexity while maintaining superior image quality, making it a viable alternative for real-time applications. Additionally, this method mitigates the challenges associated with single plane wave imaging by improving the suppression of sidelobe artifacts and enhancing image clarity without requiring multiple wave transmissions.

In different single plane wave reconstruction methods, the underlying network maps the input plane wave data at different angles, uniformly, to the base image. However, the data will be quite different from each other at different input angles. Therefore, it can cause computational problems during network training. Most discussed methods either ignore this problem or fix the plane wave transmission angle to zero degree when training the network. In another study of Zhou et al. (2018) [43], a cGAN was used to learn the mapping between 1500 single plane wave RF data from a database and 75 plane wave composite images. To solve the problem of angles, it was proposed to reconstruct an image of a single plane wave at any arbitrary transmission angle like the image of composite 75 angles using a multiscale CNN. They used 75 different versions of a multiscale CNN such that each network was trained using RF data corresponding to a unique angle. The data used are from the PICMUS and CPWC datasets.

Wasih et al. (2023) [44] proposed a cascaded deep neural network approach to reconstruct an ultrasound image from a plane wave. To solve the problem of data variability in different angles, a linear data transformation technique was used to equalize the data in different angles to zero degrees. Instead of using many identical networks for each angle, a data transformation technique was used to make the input data as similar as possible. This process results in a DNN network that requires less memory and time. The transformed input data is then used to train CNN. This network, called PixelNet, learns the weight of pixels, which is then multiplied in the single-angle DAS image. The images obtained after PixelNet are then used to train a cGAN to further reduce the noise from the image. The networks were trained on the publicly available PICMUS and CPWC datasets and evaluated on a separate CUBDL dataset obtained from different acquisition settings than the training dataset. Fig. 27 displays the complete CPWI image compared to the results of different beamforming methods of a single plane wave steered at +3.02.

Jui-Ying Lu et al. (2022) [45] introduced a novel convolutional neural network (CNN)-based beamforming approach to enhance the quality of single-angle plane wave ultrasound imaging. Traditional methods like Delay-and-Sum (DAS) beamforming often result in a tradeoff between image quality and frame rate, particularly in single-angle plane wave imaging. The authors developed a CNN beamformer that combines GoogLeNet and U-Net architectures to replace the conventional DAS algorithm. This model uses RF channel data as input and outputs in-phase and quadrature data, enabling high-quality image reconstruction. Simulations and phantom experiments demonstrated that the CNN beamformer significantly improved resolution and contrast compared to DAS. In in vivo studies, the contrast-to-noise ratio (CNR) of carotid artery images produced by the CNN beamformer was approximately 12 dB, much higher than the 3.9 dB achieved by DAS. The CNN beamformer effectively preserved tissue speckle details while minimizing the tradeoff between image quality and frame rate inherent in coherence compounding.

To improve single angle plane wave ultrasound imaging, Xiaolei Qu et al. (2023) [46] presented an innovative approach. The authors propose a transformer-

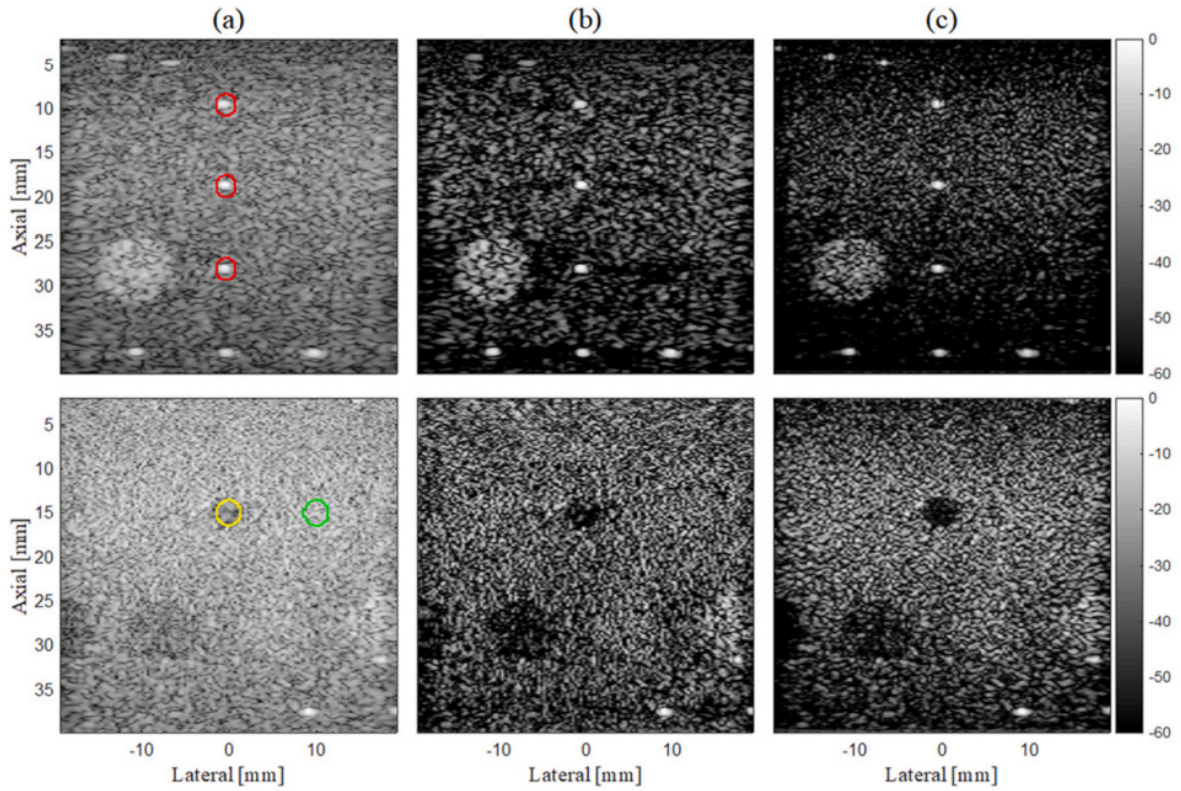

Fig 26. PW phantom simulation images using (a) DAS, (b) MV, and (c) ABF-MV [41]

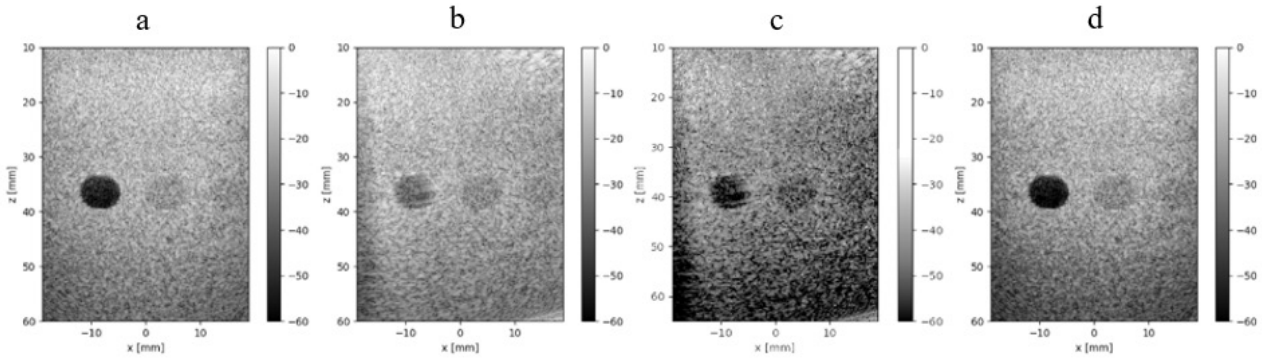

Fig 27. (a) shows the ground-truth image (full CC). (b), (c), and (d) were obtained by different methods using a single plane wave steered at +3.02. (b) shows the image made by DAS, (c) was obtained using MV, and (d) displays the image obtained by the proposed method [44].

based deep learning model that effectively captures both global and local features of ultrasound data. This complex transformer network is designed to address the challenges of low image quality and limited resolution associated with single-angle plane-wave imaging. By leveraging the attention mechanism inherent in transformers, the method enhances image reconstruction accuracy and achieves superior image quality compared to traditional techniques.

Viñals et al. (2024) [47] conducted a comparative analysis of convolutional neural networks (CNNs) trained on radiofrequency (RF) versus IQ data to enhance the quality of ultrafast ultrasound imaging. Their findings indicate that training CNNs with RF data can yield superior improvements in image quality, demonstrating the potential of RF-based training for advanced image reconstruction. Additionally, the study by Huang et al. (2024) [48] focuses on improving the quality of ultrafast ultrasound imaging using advanced deep learning techniques. The authors propose a 3D deep convolutional neural network (3D-CNN) framework specifically designed to enhance the quality of 3D ultrafast ultrasound images. This method addresses common challenges such as noise and artifacts, which are prevalent in high-frame-rate

imaging. By leveraging the spatial and temporal information inherent in 3D data, the proposed approach achieves significant improvements in image clarity and diagnostic reliability.

6 Discussion

In this article, we aimed to review the research conducted in the field of increasing the frame rate in ultrasound imaging. Table 2 presents the articles and methods investigated in this study. We reviewed various medical ultrasound imaging methods, starting with conventional imaging with linear and phased arrays in part 2. Due to its low frame rate, methods were designed to increase the imaging speed, which we mentioned in part 2.1. These methods are divided into three categories: data acquisition schemes, post-processing methods, and beamforming, each study may have one of these approaches. We mentioned several methods, including retrospective gating, matching with ECG, and various interpolation methods. These methods face challenges, especially in cases of irregular heartbeats. Another way to increase the frame rate is to record a percentage of lines and then reconstruct other data using compressed sensing (CS), but this method has high computational complexity. Other methods based on DCT, and matrix completion (MC) were also discussed to overcome these challenges.

Part 3 introduced synthetic aperture (STA) imaging; to increase the frame rate, the proposed method reduces the active elements in the aperture and records a percentage of the frames and then reconstructs the other frames using tensor completion. Part 4 discussed the ultrafast imaging method, which is plane wave imaging. Due to the low image quality in this method, the plane wave combination method (CPWI) was proposed in part 4.1. However, increasing the number of angles in this method reduced the frame rate. Most solutions involve reducing the number of angles, but this leads to a decrease in image quality. Therefore, a compromise between frame rate and image quality must be made.

In some studies, the number of angles was randomly reduced, and then unrecorded frames were reconstructed using TC or interpolation methods. In another study, reduced angles were categorized into two types whose task was to create desired contrast and resolution. However, the information from unregistered angles was not recovered. We mentioned that beamforming is one way to increase speed, and in one study, all data did not take part in the MV process and were reconstructed using the TC method.

Finally, we discussed the neural network, which has recently received attention, and studies have been conducted in this field. Numerous studies have tried to convert quality from different modalities. For example, creating line-by-line imaging quality in PWI imaging or converting data quality from DAS beamforming to MV. However, there are challenges, such as paying attention to the angle at which the PW is recorded, and it is not possible to train and test the data of one angle with the data of another angle, so all angles must be mapped to a single angle. Another challenge is the movement of the tissue, the studies conducted on the fixed tissue or the movement in the tissue such as the carotid artery have been omitted. However, these methods are not applicable to the moving tissue of the heart. Another issue is that the training data is from normal and healthy tissue, and the question that arises is that in the process of testing and exploitation if, for example, an image containing a tumor is given to the network, the tumor may not be detected and removed. So, there should be a rich dataset of all diseases that can train the network powerfully for different conditions.

7 Conclusion

In conclusion, increasing the frame rate of cardiac imaging is one area where researchers are still looking for ways to increase the speed to cover the rapid movements of the heart and capture excellent quality and comprehensive images for both healthy and diseased subjects. This article is a review of researches that were done from different perspectives. Some with acquisition, some with post-processing and some with beamforming. Methods that focus on increasing speed through the data acquisition process have more reliability than post-processing methods that aim at reconstruction through existing data. Today, research on the use of neural networks has gained strength. In this method, a network is used that trains low-quality PW input with high-quality data, and in this way, you can get a quality like the combination of 75 angles from one angle. Some points here are important and should be considered, including the data set used, which should be large enough and in such a way that the network can be trained well. In the data that has been used, the subject of disease and abnormal tissue conditions have not been considered, and generally they have been recorded from healthy and normal people. As a result, the network will not be able to recognize abnormal images, and if such an image is given to the network, it will probably erase the abnormal factors of the image. As a result, it cannot be used to diagnose diseases in practice. Here comes the importance of educational data. And if such a collection is created, such separation should also be considered in the networks so that they can receive different images and according to the type of disease, training and testing can be done in the desired category. With this assumption, there is still a challenging way for researchers.

Table 2. The studies mentioned in this article about increasing the frame rate of ultrasound imaging.

Authors, ref, Year	Acquisition Technique	Application	Approach	Method	Temporal Enhancement
Wang et al. [13] (2008)	Multi-line acquisition, multi-line transmission, (Phased array)	B-mode Cardiac imaging	Acquisition, post-processing	Retrospective ECG gating	481 Hz
Gifani et al. [15] (2010)	Conventional Phased array	B-mode Cardiac imaging	post-processing	Manifold learning	3-fold
Perrin et al. [14] (2012)	Conventional Phased array	B-mode Cardiac imaging	Acquisition, post-processing	ECG gating	3-fold
Gifani et al. [18] (2015)	Conventional Phased array	B-mode Cardiac imaging	post-processing	Interpolation, IVTC curves, Sparse representation	ratios: 1.4, 1.8, 2, 2.4, and 3
Zhou et al. [42] (2018)	PWI imaging (Linear array)	PICMUS & CPWC data	post-processing	Neural Networks (cGAN, CNN)	One PWI to 75-CPWI
Zhou at el. [39] (2019)	PWI imaging Linear imaging (Linear array)	carotid artery	post-processing	Neural Networks (GAN) Reconstructing one PWI image into a line scan image comparable to the 75-CPWI	75-fold
Hosseinpour et al. [26] (2019)	Conventional Linear/Phased array	2D carotid artery, 3D simulated Echocardiography	Acquisition	Compressed Sensing (CS), IVTC curves,	2-fold
Afrakhteh et al. [27] (2020)	Conventional Linear/Phased array	Simulated cyst phantom, Cardiac imaging	Acquisition	DCT-based reconstruction	33% of line
Hosseinpour et al. [28] (2020)	Conventional Linear/Phased array	2D carotid artery, 3D simulated Echocardiography	Acquisition	Matrix Completion (MC)	2-fold
Mirarkolaei et al. [21] (2020)	Conventional Phased array	B-mode Cardiac imaging	post-processing	Motion-compensated frame interpolation using Euler-Lagrange equations	2-fold
Jalali et al. [22] (2020)	Conventional Phased array	B-mode Cardiac 3D imaging	post-processing	IVTC curves, interpolation using cubic B-splines	orders: 1, 2,3, 4, 5, 6
Afrakhteh et al. [30] (2021)	synthetic aperture (STA) imaging	Simulated point/cyst target, experimental phantom	Acquisition	Tensor Completion (TC)	3-fold
Afrakhteh et al. [34] (2021)	CPWI imaging (Linear array)	Simulated/ experimental point/ cyst targets, carotid artery. (PICMUS data)	Acquisition	Tensor Completion (TC)	20% coherent plane waves
Tang et al. [40] (2021)	PWI imaging (Linear array)	PICMUS data	post-processing	Neural Networks (GAN) Reconstructing one PWI image into 75-CPWI	75-fold
Wang et al. [41] (2022)	PWI imaging (Linear array)	Simulated/ experimental point/ cyst targets, carotid artery.	post-processing	Neural Networks, DAS-beamformed image reconstruction to MV-beamformed image	1000 fps
Afrakhteh [31] (2022)	Conventional Linear/Phased array	Simulated cyst target, Cardiac imaging	Acquisition	Tensor Completion (TC)	4-fold
Jalilian et al. [25] (2023)	Conventional Phased array	2D/3D echocardiography	post-processing	spatial-temporal numerical method, IVTS curves, 2D interpolation, Radial Basis Functions (RBFs)	ratios: 2, 3, 4
Afrakhteh et al. [35,36] (2023)	CPWI imaging (Linear array)	PICMUS data	Acquisition	2D spatial-angular interpolation, Radial Basis Functions (RBFs)	33% coherent plane waves (25, 50 of 75)
Paridar et al. [33] (2023)	CPWI imaging (Linear array)	PICMUS data	post-processing	MV algorithm based on tensor completion (TC)	40% of the data

Paridar et al. [38] (2023)	CPWI imaging (Linear array)	PICMUS data	Acquisition	Reducing the number of angels with an optimal value	16 transmissions (of 75)
Wasih at el. [43] (2023)	PWI imaging (Linear array)	PICMUS & CPWC & CUBDL data	post-processing	Cascaded Deep Neural Networks (cGAN, DNN, CNN)	Increasing the quality/speed of a PWI by converting DAS quality to MV and making it comparable to CPWI

References

[1] J. E. Aldrich, "Basic physics of ultrasound imaging," Critical care medicine, vol. 35, no. 5, pp. S131-S137, 2007.

[2] F. Guidi and P. Tortoli, "Real-time high frame rate color flow mapping system," IEEE Transactions on Ultrasonics, Ferroelectrics, and Frequency Control, vol. 68, no. 6, pp. 2193-2201, 2021.

[3] J. A. Jensen, "Medical ultrasound imaging," Progress in biophysics and molecular biology, vol. 93, no. 1-3, pp. 153-165, 2007.

[4] D. Q. Le, E. Chang, P. A. Dayton, and K. Johnson, "High-framerate dynamic contrast-enhanced ultrasound imaging of rat kidney perfusion," in 2019 IEEE International Ultrasonics Symposium (IUS), 2019: IEEE, pp. 1326-1329.

[5] H. Huang, G. Bustamante, R. Peterson, and J. Y. Ye, "An adaptive filtered back-projection for photoacoustic image reconstruction," Medical physics, vol. 42, no. 5, pp. 2169-2178, 2015.

[6] M. Pramanik, "Improving tangential resolution with a modified delay-and-sum reconstruction algorithm in photoacoustic and thermoacoustic tomography," Journal of the Optical Society of America A, vol. 31, no. 3, pp. 621-627, 2014.

[7] J. A. Jensen, "Ultrasound imaging and its modeling," in Imaging of complex media with acoustic and seismic waves: Springer, 2002, pp. 135-166.

[8] M. Schickert, M. Krause, and W. Müller, "Ultrasonic imaging of concrete elements using reconstruction by synthetic aperture focusing technique," Journal of materials in civil engineering, vol. 15, no. 3, pp. 235-246, 2003.

[9] J. Bercoff, "Ultrafast ultrasound imaging," Ultrasound imaging-Medical applications, pp. 3-24, 2011.

[10] D. P. Shattuck, M. D. Weinshenker, S. W. Smith, and O. T. von Ramm, "Explososcan: A parallel processing technique for high speed ultrasound imaging with linear phased arrays," The Journal of the Acoustical Society of America, vol. 75, no. 4, pp. 1273-1282, 1984.

[11] R. Mallart and M. Fink, "Improved imaging rate through simultaneous transmission of several ultrasound beams," in New Developments in Ultrasonic Transducers and Transducer Systems, 1992, vol. 1733: SPIE, pp. 120-130.

[12] M. Cikes, L. Tong, G. R. Sutherland, and J. D'hooge, "Ultrafast cardiac ultrasound imaging: technical principles, applications, and clinical benefits," JACC: Cardiovascular Imaging, vol. 7, no. 8, pp. 812-823, 2014.

[13] S. Wang, W.-N. Lee, J. Provost, J. Luo, and E. E. Konofagou, "A composite high-frame-rate system for clinical cardiovascular imaging," IEEE transactions on ultrasonics, ferroelectrics, and frequency control, vol. 55, no. 10, pp. 2221-2233, 2008.

[14] D. P. Perrin, N. V. Vasilyev, G. R. Marx, and P. J. del Nido, "Temporal enhancement of 3D echocardiography by frame reordering," JACC: Cardiovascular Imaging, vol. 5, no. 3, pp. 300-304, 2012.

[15] P. Gifani, H. Behnam, and Z. A. Sani, "A new method for pseudo-increasing frame rates of echocardiography images using manifold learning," Journal of Medical Signals & Sensors, vol. 1, no. 2, pp. 107-112, 2011.

[16] P. Gifani, H. Behnam, A. Shalbaf, and Z. A. Sani, "Automatic detection of end-diastole and end-systole from echocardiography images using manifold learning," Physiological measurement, vol. 31, no. 9, p. 1091, 2010.

[17] A. Shalbaf, Z. AlizadehSani, and H. Behnam, "Echocardiography without electrocardiogram using nonlinear dimensionality reduction methods," Journal of Medical Ultrasonics, vol. 42, pp. 137-149, 2015.

[18] P. Gifani, H. Behnam, F. Haddadi, Z. A. Sani, and M. Shojaeifard, "Temporal super resolution enhancement of echocardiographic images based on sparse representation," IEEE transactions on ultrasonics, ferroelectrics, and frequency control, vol. 63, no. 1, pp. 6-19, 2015.

[19] M. Alessandrini et al., "A new technique for the estimation of cardiac motion in echocardiography based on transverse oscillations: A preliminary evaluation in silico and a feasibility demonstration in vivo," IEEE Transactions on Medical Imaging, vol. 33, no. 5, pp. 1148-1162, 2014.

[20] M. Alessandrini et al., "Detailed evaluation of five 3D speckle tracking algorithms using synthetic echocardiographic recordings," IEEE transactions on medical imaging, vol. 35, no. 8, pp. 1915-1926, 2016.

[21] H. N. Mirarkolaei, S. R. Snare, A. H. S. Solberg, and E. N. Steen, "Frame rate up-conversion in cardiac ultrasound," Biomedical Signal Processing and Control, vol. 58, p. 101863, 2020.

[22] M. Jalali, H. Behnam, F. Davoodi, and M. Shojaeifard, "Temporal super-resolution of 2D/3D echocardiography using cubic B-spline interpolation," Biomedical Signal Processing and Control, vol. 58, p. 101868, 2020.

[23] M. Jalali and H. Behnam, "Speckle tracking accuracy enhancement by temporal super-resolution of three-dimensional echocardiography images," Journal of Medical Signals & Sensors, vol. 11, no. 3, pp. 177-184, 2021.

[24] S. Afrakhteh, H. Jalilian, G. Iacca, and L. Demi, "Temporal super-resolution of echocardiography using a novel high-precision non-polynomial interpolation," Biomedical Signal Processing and Control, vol. 78, p. 104003, 2022.

[25] H. Jalilian, S. Afrakhteh, G. Iacca, and L. Demi, "Increasing frame rate of echocardiography based on a novel 2d spatio-temporal meshless interpolation," Ultrasonics, vol. 131, p. 106953, 2023.

[26] M. Hosseinpour, H. Behnam, and M. Shojaeifard, "Temporal super resolution of ultrasound images using compressive sensing," Biomedical Signal Processing and Control, vol. 52, pp. 53-68, 2019.

[27] S. Afrakhteh and H. Behnam, "A fast and high frame rate adaptive beamforming using DCT-based RF-line recovery in line-by-line ultrasound imaging," International Journal of Imaging Systems and Technology, vol. 30, no. 4, pp. 1080-1094, 2020.

[28] M. Hosseinpour, H. Behnam, and M. Shojaeifard, "Temporal Super-resolution of Ultrasound Imaging Using Matrix Completion," Ultrasonic Imaging, vol. 42, no. 3, pp. 115-134, 2020.

[29] S. I. Nikolov, Synthetic aperture tissue and flow ultrasound imaging. Center for Fast Ultrasound Imaging, Technical University of Denmark Lyngby, 2002.

[30] S. Afrakhteh and H. Behnam, "Efficient synthetic transmit aperture ultrasound based on tensor completion," Ultrasonics, vol. 117, p. 106553, 2021.

[31] S. Afrakhteh, G. Iacca, and L. Demi, "High Frame Rate Ultrasound Imaging by Means of Tensor Completion: Application to Echocardiography," IEEE Transactions on Ultrasonics, Ferroelectrics, and Frequency Control, vol. 70, no. 1, pp. 41-51, 2022.

[32] E. Macé, G. Montaldo, I. Cohen, M. Baulac, M. Fink, and M. Tanter, "Functional ultrasound imaging of the brain," Nature methods, vol. 8, no. 8, pp. 662-664, 2011.

[33] G. Montaldo, M. Tanter, J. Bercoff, N. Benech, and M. Fink, "Coherent plane-wave compounding for very high frame rate ultrasonography and transient elastography," IEEE transactions on ultrasonics, ferroelectrics, and frequency control, vol. 56, no. 3, pp. 489-506, 2009.

[34] S. Afrakhteh and H. Behnam, "Coherent plane wave compounding combined with tensor completion applied for ultrafast imaging," IEEE Transactions on Ultrasonics, Ferroelectrics, and Frequency Control, vol. 68, no. 10, pp. 3094-3103, 2021.

[35] S. Afrakhteh, H. Jalilian, G. Iacca, and L. Demi, "Application of a 2D interpolation technique to reduce the number of steering angles required for high-quality ultrasound images in plane-wave compounding," The Journal of the Acoustical Society of America, vol. 153, no. 3_supplement, pp. A353-A353, 2023.

[36] S. Afrakhteh, G. Iacca, and L. Demi, "High Contrast and High Frame Rate Coherent Plane Wave Compounding by Means of 2D Spatio-Angular Interpolation Technique," in 2023 IEEE International Ultrasonics Symposium (IUS), 2023: IEEE, pp. 1-4.

[37] R. Paridar and B. M. Asl, "Ultrafast Plane Wave Imaging Using Tensor Completion–Based Minimum Variance Algorithm," Ultrasound in Medicine & Biology, vol. 49, no. 7, pp. 1627-1637, 2023.

[38] R. Paridar and B. M. Asl, "Frame rate improvement in ultrafast coherent plane wave compounding," Ultrasonics, vol. 135, p. 107136, 2023.

[39] Z. Zhou, Y. Wang, Y. Guo, X. Jiang, and Y. Qi, "Ultrafast plane wave imaging with line-scan-quality using an ultrasound-transfer generative adversarial network," IEEE journal of biomedical

and health informatics, vol. 24, no. 4, pp. 943-956, 2019.

[40] J. Tang, B. Zou, C. Li, S. Feng, and H. Peng, "Plane-wave image reconstruction via generative adversarial network and attention mechanism," IEEE Transactions on Instrumentation and Measurement, vol. 70, pp. 1-15, 2021.

[41] W. Wang, Q. He, Z. Zhang, and Z. Feng, "Adaptive beamforming based on minimum variance (ABF-MV) using deep neural network for ultrafast ultrasound imaging," Ultrasonics, vol. 126, p. 106823, 2022.

[42] L. S. Nguon, J. Seo, K. Seo, Y. Han, and S. Park, "Reconstruction for plane-wave ultrasound imaging using modified U-Net-based beamformer," Computerized Medical Imaging and Graphics, vol. 98, p. 102073, 2022.

[43] Z. Zhou, Y. Wang, J. Yu, Y. Guo, W. Guo, and Y. Qi, "High spatial–temporal resolution reconstruction of plane-wave ultrasound images with a multichannel multiscale convolutional neural network," IEEE transactions on ultrasonics, ferroelectrics, and frequency control, vol. 65, no. 11, pp. 1983-1996, 2018.

[44] M. Wasih, S. Ahmad, and M. Almekkawy, "A robust cascaded deep neural network for image reconstruction of single plane wave ultrasound RF data," Ultrasonics, vol. 132, p. 106981, 2023.

[45] J.-Y. Lu, P.-Y. Lee, and C.-C. Huang, "Improving image quality for single-angle plane wave ultrasound imaging with convolutional neural network beamformer," IEEE Transactions on Ultrasonics, Ferroelectrics, and Frequency Control, vol. 69, no. 4, pp. 1326-1336, 2022.

[46] X. Qu et al., "Complex transformer network for single-angle plane-wave imaging," Ultrasound in Medicine & Biology, vol. 49, no. 10, pp. 2234-2246, 2023.

[47] R. Viñals, P. Motta, and J.-P. Thiran, "Enhancement of Ultrafast Ultrasound Images: a Performance Comparison Between CNN Trained with RF or IQ Images," in 2024 IEEE Ultrasonics, Ferroelectrics, and Frequency Control Joint Symposium (UFFC-JS), 2024: IEEE, pp. 1-4.

[48] H. Huang, Y. Zhao, Z. Zhou, D. Zhu, F. Varray, and H. Liebgott, "3D Ultrafast Ultrasound Image Quality Enhancement using 3D Deep Convolutional Neural Networks," in 2024 IEEE Ultrasonics, Ferroelectrics, and Frequency Control Joint Symposium (UFFC-JS), 2024: IEEE, pp. 1-4.

Biographies

Seyyedeh Ensiyeh Hashemi received the B.S. degree in Telecommunication Electrical Engineering from University of Qom, Iran in 2014, and the M.S. degree in Biomedical Engineering from Amirkabir University, Tehran, Iran in 2018. She is currently pursuing her Ph.D. in Electronic Engineering at Iran University of Science and Technology (IUST), Tehran, Iran. Her research interests include medical ultrasound imaging, image and signal processing.

Hamid Behnam received the B.S. degree in Electrical Engineering from IUST, Tehran, Iran, in 1988, the M.S. degree in medical engineering from Sharif University of Technology, Tehran, Iran, in 1992, and the Ph.D. degree in applied electronics from Tokyo Institute of Technology, Tokyo, Japan, in 1998. Since 1998, he has been a Researcher with Iran Research Organization for Science and Technology, Tehran, Iran. Currently, he is an Associate Professor of Biomedical Engineering with IUST. His research interests include ultrasound in medicine, medical image processing, and medical signal processing.